# NUMERICAL SIMULATION OF $CO_2$ FLOWS IN PIPES WITH PHASE TRANSITION ACROSS THE TRIPLE POINT

Sergey Martynov[a], Wentian Zheng[a], Solomon Brown[b] and Haroun Mahgerefteh[a,*]
[a]Department of Chemical Engineering, University College London, London WC1E7JE, UK
[b]Department of Chemical and Biological Engineering, University of Sheffield, Mappin Street, S1 3JDUK
*Author for correspondence
E-mail: h.mahgerefteh@ucl.ac.uk

## ABSTRACT

The formation of solid $CO_2$, commonly known as 'dry ice', resulting from the near-isentropic expansion of $CO_2$ to pressures below its triple point (5.18 bar), is of significant practical importance for the design and safe operation of various systems utilising high-pressure $CO_2$, including transportation pipelines and vessels, as well as cryogenic and cleaning devices. In the present study, a compressible flow Computational Fluid Dynamics (CFD) model is developed to predict the formation of dry ice during a transient decompression of $CO_2$ pipelines. The model is based on the Homogeneous Equilibrium Mixture (HEM) assumption and utilizes an extended Peng-Robinson equation of state to predict the physical properties of $CO_2$ in vapour, liquid and solid states. To ensure hyperbolicity of the flow equations the frozen speed of sound model is applied to the solid-liquid-vapour mixtures at the thermodynamic triple point of $CO_2$. The developed model is validated against the pressure and temperature measurements obtained in a full-bore rupture test performed using a 144 m long 150 mm diameter pipeline, initially filled with dense phase $CO_2$ at 153.3 bar and 5.25 $^oC$. The results of simulation show that the total amount of dry ice found in the pipeline at the end of decompression process is *ca* 12 kg, which corresponds to 0.48% of the initial inventory of the pipe.

## NOMENCLATURE

| | | |
|---|---|---|
| $C$ | [J/kg·K] | Heat capacity of the pipe wall |
| $c$ | [m/s] | Sound speed |
| $D$ | [m] | Pipeline inner diameter |
| $E$ | [J/kg] | Specific total energy of the mixture |
| $e$ | [J/kg] | Specific internal energy |
| $f$ | [-] | Fanning friction factor |
| $h$ | [W/(m$^2$K)] | Overall heat transfer coefficient |
| $p$ | [bar] | Pressure |
| $q$ | [W/m$^2$] | Heat flux at the pipe wall |
| $s$ | [J/kg·K] | Specific entropy |
| $t$ | [s] | Time |
| $u$ | [m/s] | Velocity |
| $v$ | [m$^3$/kg] | Specific volume |
| $z$ | [m] | Pipeline axial coordinate |
| $x_k$ | [-] | Mass fraction of phase $k$ |

Special characters

| | | |
|---|---|---|
| $\alpha$ | [-] | Volume fraction ratio |
| $\delta$ | [m] | Pipeline wall thickness |
| $\rho$ | [kg/m$^3$] | Density |

Subscripts

| | |
|---|---|
| $f$ | Forced convection heat transfer |
| $nb$ | Nucleate boiling heat transfer |
| $k$ | Phase index |
| $l$ | Liquid phase |
| $v$ | Vapour phase |
| $s$ | Solid phase/saturated phase |
| $w$ | Pipeline wall |

## INTRODUCTION

Recent appreciation of the impact of greenhouse gas emissions on global warming has resulted in the development of a number of decarbonisation strategies aiming to reduce the amount of carbon dioxide ($CO_2$) emissions into the atmosphere from fossil-fuel based industries [1]. Central to this strategy is Carbon Capture and Sequestration (CCS) technology which aims to capture $CO_2$ and store it in geological formations [2], and also Carbon Capture and Utilisation (CCU) where $CO_2$ is considered as a raw material for producing value-added chemicals and fuels [3]. Along with these two schemes, there is a considerable interest in optimising processes where $CO_2$ is used as conventional working fluid, e.g. in cleaning, refrigeration, heat exchangers and power cycles [4]–[7].

In order to ensure the safe design of systems utilising $CO_2$ as a compressed gas, saturated liquid or supercritical fluid, the potential risks associated with asphyxiation by $CO_2$ released in a confined environment [8] and rupture of high-pressure $CO_2$ vessels and pipes [9], [10], should be adequately assessed. Apart from these hazards, formation of dry ice upon expansion of $CO_2$ fluid brings extra risks associated with the blockage to the flow and pressure relief safety valves [11], erosional impact of dry ice particles on adjacent equipment [12] and cryogenic burns [13]. Practically, to eliminate the risk of dry ice accumulation in pressurised $CO_2$ liquid storage tanks, the tanks' minimum operating pressure is commonly set to above the $CO_2$ triple point pressure (5.18 bar) [14]. Although during emergency and venting operations of pressurised $CO_2$ vessels and pipes, the pressure may drop down to 1 bar, the exact conditions and possible amount of dry ice that may form in

such scenarios, remain largely uncertain. As such, there is a significant interest in developing models capable of predicting accurately the dry ice formation in $CO_2$ pressurised systems upon their rapid decompression.

Despite the progress in modelling decompression of pipelines and vessels carrying flashing liquids, the majority of the models have been developed for two-phase vapour-liquid flows (see, e.g. [21, 22]). However, the thermodynamics of $CO_2$ adds extra challenges to the modelling of it decompression to atmospheric pressures, which are associated with the appearance of dry ice in $CO_2$ expansion flows. In particular, the homogeneous equilibrium model predicts that the speed of sound of the solid-liquid-vapour mixture at the triple point tends to zero [15], resulting in a loss of hyperbolicity of the governing flow equations. Although this may in theory result in stagnation of the flow at the triple point [16], experimental observations of $CO_2$ decompression in vessels and pipelines [17], [18], [19] confirm the depressurisation to atmospheric pressure below the triple point of $CO_2$. In order to overcome the discontinuity in the speed of sound at the triple point, Hammer et al [20] have assumed a smooth variation in the speed of sound in the three-phase region in their HEM flow model of $CO_2$ pipeline decompression. For a hypothetical scenario of a dense-phase $CO_2$ pipeline decompression the model predicted temporary stabilisation of the flow pressure at the triple point and dry ice formation in the pipe. In a recent study by the authors [19], based on the results of simulations of $CO_2$ pipeline decompression down to triple-point pressure, it has been suggested that dry ice accumulation in the pipeline may be significant for long pipes (more than 20 km in length). However, none of the above studies have investigated in detail the dry ice formation in pipes during the decompression process.

In the present study a computational HEM model of pipeline decompression is developed accounting for finite value of the speed of sound of the $CO_2$ fluid at the triple point. The model is validated against recently published data obtained in a large-scale $CO_2$ pipeline FBR test [21] and applied to perform sensitivity analysis of the impact of heat transfer and the choice of the triple point speed of sound model on the pipeline decompression histories and the dynamics of the flow in the pipeline upon transition across the triple point.

## PIPELINE DECOMPRESSION MODEL

In this work, to describe the transient multiphase flow evolving as a result of decompression of dense-phase $CO_2$ in a pipeline, a one-dimensional model assuming the thermodynamic and mechanical equilibrium between the fluid phases (i.e. assuming the homogeneous equilibrium mixture (HEM) is applied. The mass, momentum and energy conservations of the HEM flow are given by [22]:

$$\frac{\partial \rho}{\partial t} + \frac{\partial \rho u}{\partial z} = 0 \tag{1}$$

$$\frac{\partial \rho u}{\partial t} + \frac{\partial \rho u^2 + p}{\partial z} = -\frac{2 f \rho u^2}{D} \tag{2}$$

$$\frac{\partial E}{\partial t} + \frac{\partial u(E+p)}{\partial z} = -u\frac{2 f \rho u^2}{D} + \frac{4q}{D} \tag{3}$$

where $\rho$, $u$ and $p$ are the mixture density, the flow velocity, and the fluid pressure, $D$, $f$ and $q$ are the pipe inner diameter, the Fanning friction factor calculated using Chen's correlation [23] and the heat flux at the pipe wall, while $E$ is the total energy of fluid defined as:

$$E = \rho(e + \frac{1}{2}u^2) \tag{4}$$

where $e$ is the specific internal energy of the mixture. In equation (3) the heat flux is defined as:

$$q = h_{nb}(T_w - T_{sat}) + h_f(T_{sat} - T), \tag{5}$$

where $T_w$, $T_{sat}$ and $T$ are the temperatures of the pipe wall, saturated liquid at a given pressure and the bulk fluid, while $h_{nb}$ and $h_f$ are the heat transfer coefficients due to nucleate boiling of liquid and forced convection calculated respectively using the Rohsensow's and Dittus-Boelter correlations [24]. To determine the pipe wall temperature, equation (5) is solved simultaneously with the lumped thermal capacity model for the heat conduction in the pipe wall [19]:

$$q = \rho_w C_w \delta_w \frac{\partial T_w}{\partial t} \tag{6}$$

where $\rho_w$, $C_w$ and $\delta_w$ are respectively the density, heat capacity and thickness of the pipe wall.

In order to close the set of equations (1) – (3) the initial and boundary conditions have to be specified for the pipeline. In the present study the fluid in the pipe prior to the release is assumed to be stagnant at a given pressure and temperature. At time $t$ = 0, a full-bore rupture (FBR) release is initiated at one end of the pipe where the flow is assumed to become instantaneously choked.

## FLUID PROPERTIES

The governing equations (1) – (3) describe evolution of the flow in terms of the density, $\rho$, momentum, $\rho u$, and internal energy, $E$. The internal energy and density of a multi-phase HEM mixture are defined in terms of the corresponding properties of the individual fluid phases and their mass fractions in the mixture $x_k$:

$$e = \sum_k x_k e_k \tag{7}$$

$$\frac{1}{\rho} = \sum_k \frac{x_k}{\rho_k} \tag{8}$$

where $k$ is the phase index ($k = v$, $l$ and $s$ for liquid, vapour and solid phases), while $\rho_k$ and $e_k$ at the density and specific internal energy of phases, which are calculated based on the extended Peng-Robinson equation of state previously developed by the authors [25].

As will be explained in the next section, the numerical solution of the governing equations (1) – (3) is based on the HLL approximate solver [26], which requires knowledge of the local speed of sound in the fluid. In the present study, the following "frozen" speed of sound expression [27] is adapted for both two-phase and three-phase HEM mixtures:

$$\frac{1}{\rho c^2} = \sum_{k=l,v,s} \frac{x_k}{\rho_k c_k^{\,2}} \tag{9}$$

where *c* represents the speed of sound in a mixture, while $c_k$ is the adiabatic speed of sound of phase *k*:

$$c_k = \sqrt{\left(\frac{\partial p}{\partial \rho_k}\right)_s} \tag{10}$$

It is noteworthy that, as mentioned in Introduction, the speed of sound of an HEM three-phase mixture at the triple point tends to zero [15]. This singularity in the behaviour of the speed of sound results in the loss of hyperbolicity of the flow equations at the triple point, posing a problem for resolving the flow. At the same time, in reality, any small degree of heterogeneity in the three-phase mixture would result in a finite speed of sound at the triple point. In the absence of an adequate physical model accounting for the effect of heterogeneity, equation (9) is applied in a present study as a practical means for removing the above singularity.

## NUMERICAL MODEL

To solve equations (1) – (3) numerically, a Finite Volume Method (FVM) is applied [28]. In this method the flow domain is firstly discretised into a number of equally spaced computational cells of width $\Delta z$, to obtain semi-discrete analogues of the governing equations, and the operator-splitting method is applied to treat various terms in the these equations [28]. The conservative spatial-derivative terms are resolved using Godunov-type flux differencing scheme combined with the HLL approximate Riemann solver [26], and the solution is advanced in time using an explicit Euler method. This is followed by integration of the non-conservative and source terms in equations (1) – (3) using a combination of explicit and implicit time integration schemes [29].

In the explicit Euler method, the integration time step, $\Delta t$, is selected based on the Courant-Friedrichs-Lewy (CFL) criterion, applied to ensure the numerical stability of the solution scheme:

$$CFL = \frac{\Delta t \max\left|u_i + c_i\right|}{\Delta z} \tag{11}$$

## RESULTS

In this section the developed model is validated against a pipeline decompression experiment performed in COOLTRANS project [21], where dense-phase $CO_2$, initially at 5.25 $^{o}$C (278.38 K) and 153.3 bar, was released from a 144 m long, 150 mm internal diameter and 11 mm wall thickness thermally insulated steel pipeline upon its instantaneous full-bore rupture (FBR) initiated at one end of the pipe. In the test the fluid pressure and temperature were measured at the closed end of the pipe. In order to simulate the pipeline decompression test the flow equations (1) – (3) are solved numerically on a uniform mesh with 1000 computational cells and using a CFL number of 0.5.

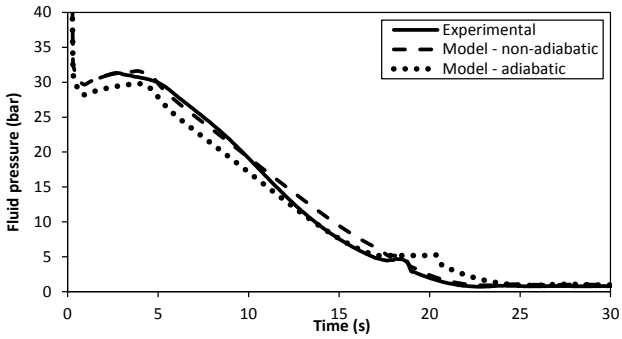


Figure 1. Fluid pressure variation with time at the closed end of the pipeline.

Figure 1 shows the pressure variation in the fluid at the back end of the pipeline as predicted by the model in comparison with the experimental data. In particular, the measured data shows that after initial rapid decrease in pressure during the liquid expansion from 153.3 bar to *ca* 30 bar, the pressure temporary stabilised for *ca* 4.5 s, which is associated with the flash-evaporation of $CO_2$ fluid. This is followed by a gradual decrease in pressure till *ca* 18 s, where the pressure stabilises near the $CO_2$ triple point (5.18 bar). As can be seen in Figure 1, these trends are reproduced by the model, which predicts the appearance of the two plateaus and their durations in a close agreement with the measurements.

In order to investigate the impact of heat transfer on the decompression flow, the simulations also have been performed using an adiabatic flow model, i.e. with $q = 0$ in equation (3). These results are also plotted in Figure 1, showing that in comparison with the model accounting for heat transfer, the adiabatic model slightly underpredicts the pressure during the first *ca* 20 s of decompression and overpredicts the pressure by a large margin at later times after passing the triple point.

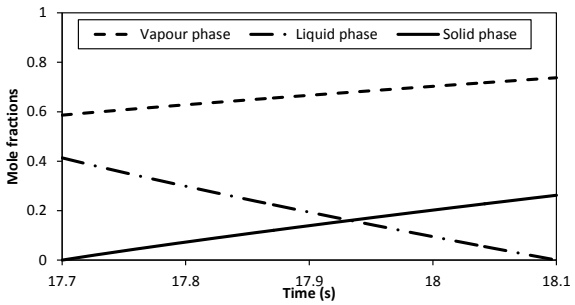


Figure 2. Predicted time variation of the fluid phase composition at the closed end of the pipeline.

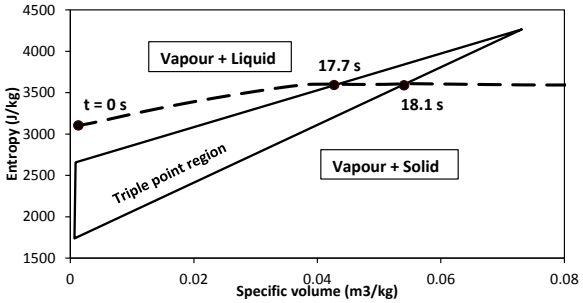


Figure 3. $s-v$ diagram of $CO_2$ showing the predicted thermodynamic trajectory of the fluid decompression at the back end of the pipe.

The predicted temporary stabilisation of pressure near the triple point is associated with the transition from the vapour-liquid equilibrium (VLE) to the solid-vapour equilibrium (SVE) mixture. This is illustrated in Figure 2 showing the variation of the phase composition in the flow at the back end of the pipe during the transition across the triple point, where the vaporisation and freezing of the liquid phase can be seen occurring at the same time. Figure 3 shows the corresponding fluid decompression trajectory plotted in the $s-v$ phase diagram, where the transition across the triple point region happens almost isentropically.

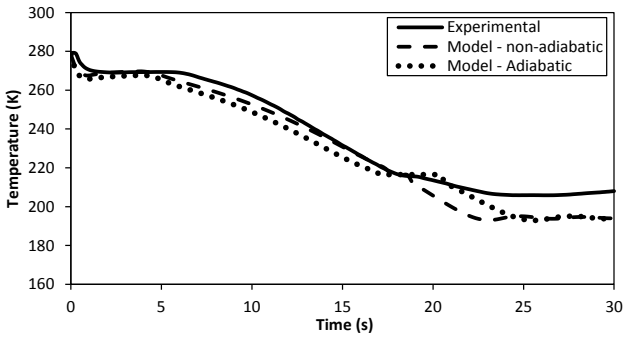


Figure 4. Fluid temperature variation with time at the closed end of the pipeline.

Figure 4 shows the model predictions and the measurements of the fluid temperature variation at the back end of the pipeline during the decompression. Here, the trends are similar to those observed in Figure 1 for the evolution of the fluid pressure. It can also be seen that during first *ca* 19 s of decompression the predictions are in close agreement with the experimental data, while the non-adiabatic flow model predicts slightly shorter temperature plateau at the $CO_2$ triple point (216.6 K) than experimentally observed. At later times, after complete transition from vapour-liquid to vapour-solid mixture, the discrepancy between the predicted and the measured temperatures systematically increases. This can be attributed to possible precipitation of the solid phase in the lower part of the pipe cross-section, hence not affecting the readings by the thermocouple positioned in the bulk stream and temporarily exposed to warmer vapour during the late stage of depressurisation.

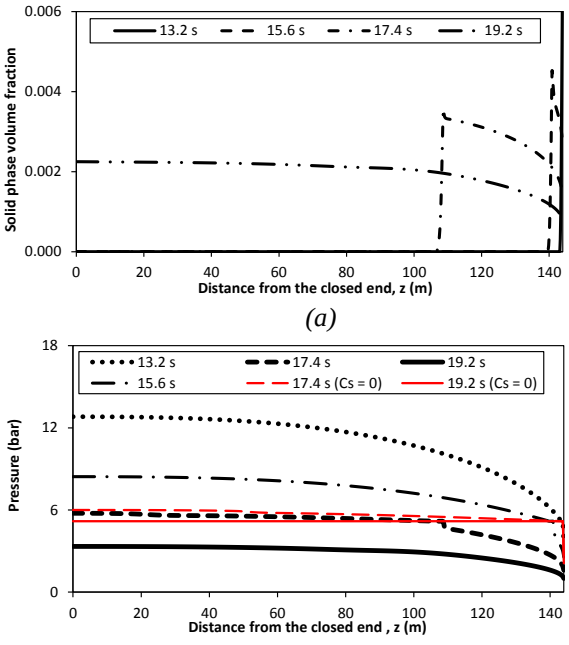


Figure 5. Variation of the solid phase volume fraction *(a)* and the fluid pressure profiles *(b)* in the pipeline at a late stage of depressurisation. Set max range for solid volume fraction to 0.006.

As mentioned in Introduction, quantification of dry ice formation in pipelines in the event of rapid decompression is of significant interest for the pipeline safe design and operation. Although the dry ice formation has not been measured directly in the COOLTRANS experiment, the developed flow model enables prediction of the amount of solid phase evolved at any time and location in the pipeline upon its decompression to pressures below the triple point. In particular, Figure 5 *a* illustrates the variation of the volume fraction of solid phase along the pipe at different times, while Figure 5 *b* shows the corresponding evolution of the fluid pressure profiles.

As can be seen in Figure 5 *a*, at 13.2 s the first appearance of the solid phase is predicted at the release end of the pipe (144 m), where the pressure dropped to 5.18 bar (Figure 5 *b*).

At the same time the fluid inside the pipe remains in a saturated vapour-liquid mixture state at pressures above 5.18 bar.

As can be further observed from Figure 5 *a*, at *ca* 15.6 s, the last 4 m of the pipe become occupied by solid-vapour mixture. The transition from liquid-vapour to a solid-vapour mixture happens in a very narrow section of the pipe where the volume fraction of the solid phase increases rapidly from zero to *ca* 35%, which is accompanied by a corresponding rapid drop in the fluid pressure (Figure 5 *b*). The steep changes in the solid phase fraction and the fluid pressure mark the location of the freezing front propagating into the pipeline. The profiles in Figure 5 *a* show that by 17.4 s the freezing front has propagated to $z$ = 108 m, while by 19.2 s the entire pipe becomes filled with solid-vapour mixture, containing *ca* 0.3% (v/v) of solid phase, which for a given the pipeline volume of *ca* 2.54 $m^3$ and density of solid phase of 1580 $kg/m^3$, translates into *ca* 12 kg of dry ice. In terms of percentage of the initial inventory, which can be estimated to be 2.49 tonne, the dry ice forms 0.48%. Given relatively large density ratio of the solid and vapour phases and low flow velocities, it is likely that the dry ice will precipitate in the pipe and gradually sublime by consuming heat from surrounding.

Returning to Figure 5 *b*, the fluid pressure rapidly drops in the direction of the flow at the location of the freezing fronts (*ca* 140 and 108 m respectively at 15.6 and 17.4 s). These step variations in pressure are associated with the dramatic changes in compressibility of the fluid undergoing the transition from the vapour-liquid to vapour-liquid-solid, and then to vapour-solid mixture at the triple point.

Figure 5 *b* also shows the pressure profiles predicted by the model assuming zero speed of sound at the triple point ($c_{tr}$ = 0). In this case after the pressure dropped to the triple point at the release end of the pipe, no further expansion of the flow and phase transition to vapour-liquid-solid mixture has been predicted. In the contrast with the predictions obtained utilising the frozen speed of sound described by equation (9), the fluid pressure equilibrates at the triple point and the total stagnation of the bulk flow is observed along the entire length of the pipe.

## CONCLUSIONS

This study presents the results of the computational modelling of dry ice formation in $CO_2$ transportation pipelines during their decompression in accidental full bore rupture scenarios. To describe the flow, a hyperbolic two-phase flow model was adapted based on the HEM fluid model applied to predict properties of the two-phase and three-phase mixtures evolving as a result of $CO_2$ expansion in the pipe. To ensure hyperbolicity of the flow equations at the triple point where the HEM speed of sound tends to zero, a frozen speed of sound correlation was applied to three-phase solid-liquid-vapour mixtures at the triple point.

The proposed flow model was validated against the pressure and temperature measurements obtained in a large-scale pipeline rupture test [21], confirming the HEM flow model capability to predict very well the FBR release scenarios involving flashing of $CO_2$ liquid from initially dense-phase state. The accuracy of the model was found to be improved when accounting for the effect of heat transfer from the pipe wall to the fluid during the decompression process. It is also shown that the developed HEM three-phase mixture model predicts the experimentally observed stabilisation of the fluid temperature and pressure during the transient phase change at the $CO_2$ triple point. The duration of the predicted period over which the pressure and temperature remained constant was found to be strongly affected by the choice of a model for calculation of the speed of sound at the triple point. In particular, setting the speed of sound to zero resulted in a full stagnation of the vapour-liquid flow at the triple point without any further decompression. In contrast, when using the frozen speed of sound at the triple point, the singularity in the HEM speed of sound was removed, and continuous decompression of the fluid in the pipeline to atmospheric pressure was predicted along with the finite durations of the pressure and temperature plateaus at the triple point.

The results of simulation of the pipeline decompression from the triple point to ambient pressure at a late stage of release showed that the model underpredicts the fluid temperature in comparison with the experimental data. The observed difference in the predicted and measured temperatures is related to possible stratification of the solid-vapour flow, which would result in the temperature difference between the solid and vapour phases and cannot be adequately described using the HEM model applied in the present study.

While the present study is focused on the prediction of conditions of dry ice formation during full-bore rupture decompression of $CO_2$ in a pipeline, analysis of scenarios of dry ice formation in pipes and vessels releasing $CO_2$ through small diameter orifices is of particular practical interest. In such scenarios stratification of $CO_2$ fluid in a pipe/vessel during the late stage of decompression [21] may have a significant impact on the temperature profiles in the fluid and, as a result, on the conditions, location and amount of dry ice formed in the system. Given the above mentioned limitation of the HEM model, assessing the ranges of its validity for predicting scenarios of dry ice formation for scenarios when the flow stratification may happen during the decompression would be of significant practical relevance. This forms part of the current authors' work, which includes validation of the flow model against experimental data and analysis of dry ice formation upon decompression of pipelines for various puncture diameters.

In order to predict the dry ice accumulation in pipes and vessels, further development of the model will be needed to account for the dry ice particles dynamics, this includes consideration of their deposition/ sedimentation during the flow.

## ACKNOWLEDGEMENTS

The research leading to this work has received funding from the European Union 7th Framework Programme FP7-ENERGY-2012-1-2STAGE under grant agreement number 309102.

## REFERENCES

[1] M. Hübler and A. Löschel, "The EU Decarbonisation Roadmap 2050—What way to walk?," *Energy Policy*, vol. 55, pp. 190–207, 2013.

[2] K. (Kailai) Thambimuthu, M. Soltanieh, J. C. Abanades, R. Allam, O. Bolland, J. Davison, P. Feron, F. Goede, A. Herrera, M. Iijima, D. Jansen, I. Leites, P. Mathieu, E. Rubin, D. Simbeck, K. Warmuzinski, M. Wilkinson, R. Williams, M. Jaschik, A. Lyngfelt, R. Span, and M. Tanczyk, "Capture of CO2," *IPCC Spec. Rep. Carbon dioxide Capture Storage*, pp. 105–178, 2005.

[3] P. Styring, D. Jansen, H. de Coninck, H. Reith, and K. Armstrong, *Carbon Capture and Utilisation in the green economy*. 2011.

[4] R. Sherman, "Carbon Dioxide Snow Cleaning," *Dev. Surf. Contam. Clean. - Fundam. Appl. Asp.*, no. 908567964, pp. 987–1012, 2008.

[5] D. Huang, G. Ding, and H. Quack, "New refrigeration system using $CO_2$ vapor-solid as refrigerant," *Front. Energy Power Eng. China*, vol. 2, no. 4, pp. 494–498, 2008.

[6] B. T. Austin and K. Sumathy, "Transcritical carbon dioxide heat pump systems: A review," *Renew. Sustain. Energy Rev.*, vol. 15, no. 8, pp. 4013–4029, 2011.

[7] M. Kim, *Fundamental process and system design issues in $CO_2$ vapor compression systems*, vol. 30, no. 2. 2004.

[8] P. Harper, J. Wilday, and M. Bilio, "Assessment of the major hazard potential of carbon dioxide ($CO_2$)," 2011.

[9] W. E. Clayton and M. L. Griffin, "Catastrophic failure of a liquid carbon dioxide storage vessel," *Process Saf. Prog.*, vol. 13, no. 4, pp. 202–209, 1994.

[10] D. Bjerketvedt, K. Egeberg, W. Ke, A. Gaathaug, K. Vaagsaether, and S. H. Nilsen, "Boiling liquid expanding vapour explosion in $CO_2$ small scale experiments," *Energy Procedia*, vol. 4, pp. 2285–2292, 2011.

[11] D. Huang, H. Quack, and G. L. Ding, "Experimental study of throttling of carbon dioxide refrigerant to atmospheric pressure," *Appl. Therm. Eng.*, vol. 27, pp. 1911–1922, 2007.

[12] M. Bilio, S. Brown, M. Fairweather, and H. Mahgerefteh, "$CO_2$ pipelines material and safety consideration. IChemE Symposium," in *HAZARDS XXI Symposium Series*, 2009, no. 155, pp. 423–429.

[13] N. J. Langford, "Carbon dioxide poisoning," *Toxicol. Rev.*, vol. 24, no. 4, pp. 229–235, 2005.

[14] Chart Inc., "$CO_2$ Storgae Tank - Product Manual," vol. 1, no. 032626, pp. 1997–2004, 2014.

[15] R. Menikoff and B. J. Plohr, "The Riemann problem for fluid flow of real materials," *Rev. Mod. Phys.*, vol. 61, pp. 75–130, 1989.

[16] S. Martynov, S. Brown, H. Mahgerefteh, and V. Sundara, "Modelling choked flow for $CO_2$ from the dense phase to below the triple point," *Int. J. Greenh. Gas Control*, vol. 19, pp. 552–558, Nov. 2013.

[17] R. Eggers and V. Green, "Pressure discharge filled with CO2," vol. 3, pp. 59–63, 1990.

[18] M. Ahmad, L. Buit, O. Florisson, and C. Hulsbosch-dam, "Experimental Investigation of $CO_2$ Outflow from a High-Pressure Reservoir," vol. 00, pp. 1–13, 2013.

[19] S. Martynov, S. Brown, H. Mahgerefteh, V. Sundara, S. Chen, and Y. Zhang, "Modelling three-phase releases of carbon dioxide from high-pressure pipelines," *Process Saf. Environ. Prot.*, vol. 92, no. 1, pp. 36–46, Jan. 2014.

[20] M. Hammer, Å. Ervik, and S. T. Munkejord, "Method using a density-energy state function with a reference equation of state for fluid-dynamics simulation of vapor-liquid-solid carbon dioxide," *Ind. Eng. Chem. Res.*, vol. 52, pp. 9965–9978, 2013.

[21] S. Brown, S. Martynov, H. Mahgerefteh, and C. Proust, "A homogeneous relaxation flow model for the full bore rupture of dense phase CO2 pipelines," *Int. J. Greenh. Gas Control*, vol. 17, pp. 349–356, Sep. 2013.

[22] H. Mahgerefteh, A. O. Oke, and Y. Rykov, "Efficient numerical solution for highly transient flows," *Chem. Eng. Sci.*, vol. 61, no. 15, pp. 5049–5056, 2006.

[23] N. H. Chen, "An Explicit Equation for Friction Factor in Pipe," *Ind. Eng. Chem. Fundam.*, vol. 18, no. 3, pp. 296–297, 1979.

[24] J. C. Chen, "Correlation for boiling heat transfer to saturated fluids in convective flow," *Ind. Eng. Chem. Process Des. Dev.*, vol. 5, pp. 322–329, 1966.

[25] S. Martynov, S. Brown, and H. Mahgerefteh, "An extended Peng-Robinson equation of state for carbon dioxide solid-vapor equilibrium," *Greenh. Gases Sci. Technol.*, vol. 3, no. 2, pp. 136–147, Apr. 2013.

[26] E. F. Toro, *Riemann Solvers and Numerical Methods for Fluid Dynamics*. 2009.

[27] D. J. Picard and P. . Bishnoi, "Calculation of the thermodynamic sound velocity in two-phase multicomponent fluids," *Int. J. Multiph. Flow*, vol. 13, no. 3, pp. 295–308, 1987.

[28] R. J. LeVeque, "Finite Volume Methods for Hyperbolic Problems," *Cambridge Univ. Press*, vol. 54, p. 258, 2002.

[29] S. Brown, S. Martynov, H. Mahgerefteh, S. Chen, and Y. Zhang, "Modelling the non-equilibrium two-phase flow during depressurisation of $CO_2$ pipelines," *Int. J. Greenh. Gas Control*, vol. 30, pp. 9–18, Nov. 2014.